

Estimation of broad-leaved canopy growth in the urban forested area using multi-temporal airborne LiDAR datasets



Youngkeun Song^{a,b,*}, Junichi Imanishi^a, Takeshi Sasaki^c, Keiko Ioki^d, Yukihiko Morimoto^e

^a Graduate School of Global Environmental Studies, Kyoto University, Kyoto, Japan

^b Graduate School of Environmental Studies, Seoul National University, Seoul, Republic of Korea

^c Graduate School of Agriculture, Kobe University, Kobe, Japan

^d Graduate School of Agriculture, Kyoto University, Kyoto, Japan

^e Faculty of Bio-environmental Science, Kyoto Gakuen University, Kyoto, Japan

ARTICLE INFO

Article history:

Received 9 March 2015

Received in revised form 6 February 2016

Accepted 17 February 2016

Available online 21 February 2016

Keywords:

Airborne laser scanning

Light detection and ranging

Remote sensing

Tree growth

Urban forest

ABSTRACT

Inter-annual canopy growth is one of the key indicators for assessing forest conditions, but the measurements require laborious field surveys. Up-to-date LiDAR remote sensing provides sufficient three-dimensional morphological information of the ground to monitor canopy heights on a broad scale. Thus, we attempted to use multi-temporal airborne LiDAR datasets in the estimation of vertical canopy growth, across various types of broad-leaved trees in a large urban park.

The growth of broad-leaved canopies in the EXPO '70 urban forest in Osaka, Japan was assessed with 19 plots at the stand level and 39 selected trees at the individual-tree level. Airborne LiDAR campaigns repeatedly observed the park in the summers of 2004, 2008, and 2010. We acquired canopy height models (CHMs) for each year from the height values of the uppermost laser returns at every 0.5 m grid. The annual canopy growth was calculated by the differences in CHMs and validated with the annual changes in field-measured basal areas and tree heights.

LiDAR estimations revealed that the average annual canopy growth from 2004 to 2010 was $0.26 \pm 0.11 \text{ m m}^{-2} \text{ yr}^{-1}$ at the plot level and $0.26 \pm 0.10 \text{ m m}^{-2} \text{ yr}^{-1}$ at the individual-tree level. This result showed that growing trends were consistent at different scales through 2004 to 2010 despite uncertainty in estimating short-term growth for small crown areas at the individual-tree level. This LiDAR-estimated canopy growth shows a moderate relation to field-measured increase of basal areas and average heights. The estimation uncertainties seem to result from the complex canopy structure and irregular crown shape of broad-leaved trees. Challenges still remain on how to incorporate the growth of understory trees, growth in the lateral direction, and gap dynamics inside the canopy, particularly in applying multi-temporal LiDAR datasets to the large-scale growth assessment.

© 2016 Elsevier GmbH. All rights reserved.

1. Introduction

Tree growth is an important indicator in assessing the vigor conditions of plants in urban forested areas. To estimate the growth, periodic fieldwork is required for the measuring increased tree heights (Hogg et al., 2005), the size of foliage (Dobbertin, 2005), stems (Poage and Tappeiner, 2002; Tappeiner et al., 1997; Waring et al., 1980), shoots (Takahashi, 2003), and roots (Reich et al., 1980)

at every single tree. However, those methods are often laborious and inefficient for large-scale surveys, and therefore the application of remote-sensing data is required.

Up-to-date airborne light detection and ranging (LiDAR) remote sensing is a highly useful method for the growth assessment of tree canopies on a large scale. The small-footprint airborne LiDAR data, which are acquired by recording three-dimensional coordinates for tens of thousands of laser pulses per second reflected from the target, provides three-dimensional morphology information of ground targets with an accuracy of dozens of centimeters. Previous studies applied this capability in the estimation of tree height (Dean et al., 2009; Næsset and Økland, 2002; Popescu, 2007), crown diameter (Popescu and Zhao, 2008), and species identification (Brandtberg, 2007; Holmgren and Persson, 2004) on the basis

* Corresponding author at: Department of Landscape Architecture, Graduate School of Environmental Studies, Seoul National University, Seoul 08826, Republic of Korea. Tel.: +82 2 880 8860; fax: +82 2 885 2096.

E-mail address: songkoon@gmail.com (Y. Song).

Table 1

Previous studies for canopy growth assessment using multi-temporal LiDAR datasets.

References	Study materials & site location	LiDAR observation years & sensors	Field campaigns & estimation scales	Accuracy/validation
St-Onge and Vepakomma (2004), Vepakomma et al. (2008, 2010, 2011)	Mixed boreal forest dominated by balsam firs, paper birch (Canada)	1998, 2003 by Optech ALTM 1020 & 2050, respectively	No field data, validation using high resolution images in 1998, 2003	Successful identification and characterization of temporal changes in forest gaps
Næsset and Gobakken (2005)	Boreal forest dominated by Norway spruce, Scots pine (Norway)	1999, 2001 both by ALTM 1210	1999 (and the tree heights in 2001 were modeled) 133 plots & 56 stands	Poor predictions by LiDAR for the modeled in-situ growth in tree height, basal area, and volume
Yu et al. (2004)	Boreal forest dominated by Norway spruce, Scots pine (Finland)	1998, 2000 both by Toposys-1	2002 (and the tree heights were estimated back to 1997) 91 trees in 3 plots & 20 stands	Discrepancy in estimating tree heights of approximately 5 cm at stand level and 10–15 cm at plot level
Yu et al. (2006)	Boreal forest dominated by Norway spruce, Scots pine (Finland)	1998, 2003 by Toposys-1 & 2, respectively	2002 (+2004, and the tree heights were estimated back to 1997) 82 trees	$R^2 = 0.681$ RMSE = 0.433 m ($N = 82$) in tree height growth
Hopkinson et al. (2008)	Temperate mature red pine plantation (Canada)	2000, 2002, 2004, 2005 by ALTM 1225, 2050, 3100 & 3100, respectively	2002, 2005 126 trees within 19 plots	Poor relationship between the growth in tree heights by field measurement and LiDAR estimation
This study	Diverse broadleaved plants in an urban forest (Fig. 1, Japan)	2004 and 2008, 2010 by ALTM 2050, Riegl LMS-Q560, respectively (Table 4)	2008, 2010 and 2012 526 trees in 19 plots at stand level, plus 39 trees at individual tree level	Successful agreement among growing rates through 6 years and moderate relationship between LiDAR-estimated height growth and increase of in-situ basal area

of LiDAR data obtained from a single operation. Accordingly, by using multiple observations of LiDAR, we could detect changes in the morphology of vegetated ground on a large scale (i.e., estimate canopy growth in wide areas) in a more accurate and efficient manner than ground survey.

Because of this potential, previous studies used multi-temporal LiDAR datasets to estimate the changes in canopy structure. Yu et al. (2004) estimated the growth of trees in boreal forests during the selected two years on the basis of the differences in two LiDAR-derived heights acquired in 1998 and 2000. Vepakomma et al. (2010, 2008) applied two LiDAR datasets to detect gap dynamics in forests, and attempted to assess tree growth not only in the vertical direction but also in the lateral direction (Vepakomma et al., 2011). However, the estimation accuracy for LiDAR-derived growth is still uncertain (Næsset and Gobakken, 2005), especially in observation intervals shorter than 3 years (Hopkinson et al., 2008). In addition, the multiple LiDAR operations may be limited by the cost for flights and the repeated laborious field surveys necessary to validate the growth. Table 1 shows that the previous studies imply limitations based on the lack of validating field data, statistically and chronologically corresponding to LiDAR observations. In addition, the targets of former studies are limited in the cases of coniferous forests. Broad-leaved canopy often shows a largely different morphology from the coniferous canopy (Koukoulas and Blackburn, 2005), having more continuous, closed, and irregular-shaped upper crowns than conifers (Song et al., 2013). Therefore, we also should highlight the morphological changes (i.e., growth assessment in this study) of the broad-leaved canopy detected by multi-LiDAR.

The goal of the study is to clarify the usefulness of multi-temporal LiDAR datasets, for the growth assessment of broad-leaved canopies. Using multiple LiDAR datasets in the summers of 2004, 2008, and 2010 for an urban park, we attempted to show the growing trends in broad-leaved canopy at the individual-tree level, as well as at the plot level. The LiDAR-estimated growth was validated with the increment of the field-measured basal area, and the potentials and uncertainties were quantified.

2. Method and materials

2.1. Study materials

The EXPO '70 Commemorative Park in Osaka, Japan (Fig. 1) was selected for this study because the forested zone in this urban park included various types of broad-leaved vegetation. Most of the trees planted on bare ground in 1972 grew well and produced a lush urban forest (Morimoto et al., 2006). Nineteen plots, dominated by broad-leaved species (Fig. 1, Table 2), were set for plot-level growth assessment from 2004 to 2010. The locations of the plots were carefully identified on the map by in-situ survey with Differential GPS instrument. For the measurement of basal areas, we selected a total of 526 trees taller than 7 m in height across all the plots. We measured the diameter at breast heights (DBHs) in 2008 and 2012, respectively, and calculated the increase of basal areas. Our assumption was that LiDAR-estimated canopy growth could be validated with the change in basal areas of those large trees. We excluded sub-canopy trees lower than 7 m because they were rarely observed from aircraft, and the height growth of those shorter trees could not be incorporated in our LiDAR-derived canopy height models (CHMs) (see Section 2.2). Field measurement of tree heights was not used for the validation of our growth results, because the accuracy of field-measured heights, especially in cases of large trees, was inadequate to compare with LiDAR measurements providing accuracy within dozens of centimeters.

In addition, we surveyed 39 flowering cherry trees (*Cerasus × yedoensis* 'Somei-yoshino') for the growth assessment at the individual-tree level (Table 3). The DBHs were measured and used to calculate basal areas in 2010 and 2012. To identify the spatial extent of individual-tree canopies, we manually drew the crown boundary polygons without mutual overlap and projected them onto the LiDAR images. Because of the irregular crown shape of deciduous broad leaves (Song et al., 2013), we could not apply the automatic crown-delineation technique (Yu et al., 2004) in this step.

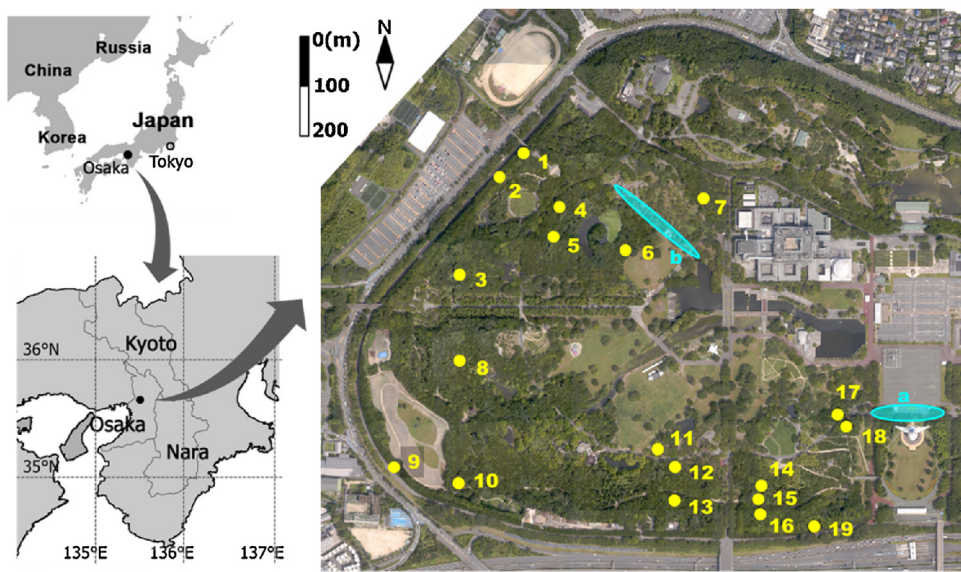


Fig. 1. Study site. In the right-hand side block, closed circles with numbers and ovals indicate the locations of plot-based (Table 2) and individual-tree-based survey (Table 3), respectively.

Table 2

Summary of field data used in the plot-based analysis (broad-leaved species dominated only N = 19).

Plot ID	Dominant species	GPS-measured area (m ²)	Assessed no. of trees	Field-measured basal area			
				2008 (m ² ha ⁻¹)	2012 (m ² ha ⁻¹)	Increase (m ² ha ⁻¹)	Increase (%)
1	<i>Quercus phillyraeoides</i> A. Gray	220.21	38	0.67	26.70	3.70	13.85
2	<i>Quercus phillyraeoides</i>	148.99	18	0.18	9.98	1.94	19.48
3	<i>Cinnamomum camphora</i> (L.) Presl, <i>Quercus glauca</i> Thunb. ex Murray	229.26	29	2.05	80.93	8.45	10.44
4	<i>Castanopsis cuspidata</i> (Thunb. ex Murray) Schottky, <i>Quercus glauca</i>	225.30	28	1.50	58.79	7.69	13.08
5	<i>Ulmus parvifolia</i> Jacquin, <i>Celtis sinensis</i> Pers. var. <i>japonica</i> (Planch.) Nakai	98.55	15	0.26	24.24	2.11	8.69
6	<i>Quercus glauca</i> , <i>Machilus thunbergii</i>	180.97	36	0.87	42.88	5.40	12.60
7	<i>Castanopsis sieboldii</i> (Makino) Hatusima ex Yamazaki et Mashiba, <i>Celtis sinensis</i> var. <i>japonica</i>	106.24	37	1.10	93.28	10.34	11.08
8	<i>Quercus glauca</i> , <i>Quercus phillyraeoides</i>	225.02	45	0.85	33.23	4.52	13.59
9	<i>Quercus phillyraeoides</i>	105.45	59	0.62	49.33	9.21	18.67
10	<i>Quercus acutissima</i> Carruthers	224.11	10	0.51	20.21	2.62	12.96
11	<i>Quercus serrata</i> Thunb. ex Murray	224.50	11	0.42	17.40	1.23	7.10
12	<i>Quercus acutissima</i> , <i>Cerasus jamaeskira</i> Sieb. ex Koidz	223.34	20	0.59	24.47	1.75	7.15
13	<i>Quercus glauca</i> , <i>Cinnamomum camphora</i>	226.25	46	1.05	41.40	5.04	12.18
14	<i>Quercus glauca</i> , <i>Ligustrum japonicum</i> Thunb.	230.72	25	0.79	29.60	4.78	16.16
15	<i>Castanopsis cuspidata</i> , <i>Machilus thunbergii</i>	230.72	21	1.08	41.11	5.71	13.88
16	<i>Machilus thunbergii</i> , <i>Quercus glauca</i>	220.89	25	0.87	35.54	3.76	10.57
17	<i>Quercus serrata</i> , <i>Prunus jamaeskira</i>	401.34	25	0.97	22.56	1.70	7.53
18	<i>Quercus serrata</i> , <i>Prunus jamaeskira</i>	406.50	10	0.35	7.99	0.69	8.65
19	<i>Cinnamomum camphora</i>	375.00	28	3.14	76.19	7.61	9.98

2.2. LiDAR data collection and processing

The LiDAR dataset was acquired by two types of airborne sensors (Table 4). The LiDAR operations were carried out three times, on October 4, 2004 by use of the ALTM 2050 (Optech Co., Ltd.) and on August 22, 2008 and August 24, 2010 by use of the LMS-Q560 (Riegl Laser Measurement Systems GmbH). The laser pulses were classified into the returns from the ground and from the canopy above

the ground by application of Terrascan software (Ver.12, Terrasolid Co., Ltd.). The ground returns were used for deriving the digital elevation model (DEM), and the above-ground canopy returns were used for digital surface model. And the CHM of each year was computed from the difference between the DEM and the digital surface model. The models in 2004, 2008, and 2010 were produced by taking the maximum z-value at every 0.5 m × 0.5 m grid from the point clouds of laser pulses in each dataset. By this CHM method

Table 3

Summary of field data used in the individual-tree-based analysis (*Cerasus × yedoensis* "Somei-yoshino", N = 39).

Crown area (m ²)	DBH(cm)				Basal area				Increase (cm ²)				Increase (%)	
	2010		2012		2010 (cm ²)		2012 (cm ²)		Mean		SD		Mean	
	Mean	SD	Mean	SD	Mean	SD	Mean	SD	Mean	SD	Mean	SD	Mean	SD
49.73	28.00	39.66	13.49	41.14	14.08	1373.64	888.13	1480.15	957.59	106.51	109.13	7.51	5.54	

Table 4

The performances of LiDAR sensors used in 2004 (Optech ALTM2050) and in 2008 and 2010 (Riegl LMS-Q560) observations.

Sensor	Optech ALTM2050	Riegl LMS-Q560
Scan angle	0±5.3°	0±30°
Beam divergence	0.19 mrad	0.5 mrad
Operating altitude	1000 m	300 m
Footprint diameter	19 cm	15 cm
Laser repetition rate	50,000 Hz	150,000 Hz
Scan frequency	67 Hz	80 Hz
Flying speed	130 kn	50 kn
Laser wavelength	1064 nm	1550 nm
The density of laser pulses	11.3 returns m ⁻²	51.8 returns m ⁻²

(Hopkinson et al., 2008; Næsset, 1997; Popescu et al., 2002), the point-clouds type of discrete LiDAR records for the canopy area was converted into the continuous raster image of upper canopy heights. We calculated the difference among the CHMs for assessing canopy growth in the vertical direction.

2.3. Growth assessment

The plot-level canopy growth was assessed on the basis of the average height, which was estimated from the mean values of each CHM within the plot boundaries in Section 2.1. The inter-annual differences in average canopy heights from CHMs were correlated with the changes in basal areas of 526 broad-leaved trees in the plots. At the individual-tree level, we obtained maximum (i.e., tree-top) and average heights of trees from CHMs, within the 39 tree-crown boundaries identified in Section 2.1. These LiDAR-derived tree heights were compared with the variation of the DBHs and basal areas from 2004 to 2008 and 2010.

3. Results

3.1. The LiDAR-measured canopy growth

The LiDAR-estimated average annual canopy growth at the plot level was $0.26 \pm 0.11 \text{ mm m}^{-2} \text{ yr}^{-1}$ from 2004 to 2010. A similar growth rate was obtained in the periods of 2008 to 2010 and 2004 to 2008 (Table 5). In the individual-tree-based estimation, the canopy grew an average of $0.26 \pm 0.10 \text{ mm m}^{-2} \text{ yr}^{-1}$ from 2004 to 2010, but

Table 6

The result of LiDAR-estimated height and annual growth at the individual-tree level.

Tree top height (m)					
2004		2008		2010	
Mean	SD	Mean	SD	Mean	SD
8.36	1.28	8.58	1.10	8.83	1.12
Average crown height (m)					
2004		2008		2010	
Mean	SD	Mean	SD	Mean	SD
3.85	0.85	5.34	1.09	5.38	1.18
Growth of crown per year ($\text{mm m}^{-2} \text{ yr}^{-1}$)					
2004–2010		2008–2010		2004–2008	
Mean	SD	Mean	SD	Mean	SD
0.26	0.10	0.02	0.19	0.37	0.14

Table 7

Pearson *r* of canopy growth in the vertical direction during study periods.

Growth	Plot level (<i>N</i> =19)		Individual tree level (<i>N</i> =39)	
	2004–2010	2008–2010	2004–2010	2008–2010
2008–2010	0.922	–	0.462	–
2004–2008	0.986	0.846	0.806	–0.153

Note: All the correlations were significant at $p<0.01$ level except for the character in gray.

the growth rate in shorter periods was $0.02 \pm 0.19 \text{ mm m}^{-2} \text{ yr}^{-1}$ and $0.37 \pm 0.14 \text{ mm m}^{-2} \text{ yr}^{-1}$ during 2008–2010 and 2004–2008, respectively (Table 6).

The plot-level growth during the periods of 2004–2008, 2008–2010, and 2004–2010 were strongly correlated with one another ($r>0.8$, $p<0.01$, $N=19$) (Table 7, Fig. 2a). At the scale of individual trees, the growth trend was not clear for every period (Table 7), although the growth during 2004–2010 was highly correlated with the 2004–2008 growth ($r=0.806$, $p<0.01$, $N=39$; Fig. 2b).

Table 5

The result of LiDAR-estimated height and growth at the plot level.

Plot ID (Table 2)	Average height (m)			Average growth (m)		
	2004	2008	2010	2004–2010	2008–2010	2004–2008
1	10.02	10.74	11.16	1.14	0.42	0.72
2	10.17	11.54	12.08	1.90	0.54	1.36
3	14.49	16.37	17.22	2.73	0.86	1.87
4	13.10	14.34	15.03	1.93	0.69	1.24
5	10.07	10.86	11.25	1.18	0.39	0.78
6	12.45	13.61	14.18	1.73	0.57	1.16
7	13.92	14.97	15.48	1.56	0.51	1.06
8	8.96	10.54	11.35	2.39	0.81	1.58
9	10.50	11.71	12.14	1.65	0.43	1.22
10	12.74	14.73	15.60	2.86	0.87	1.99
11	10.18	10.44	10.57	0.38	0.13	0.25
12	14.52	14.84	15.15	0.63	0.31	0.32
13	11.43	11.91	12.20	0.77	0.29	0.48
14	11.36	12.11	12.84	1.48	0.73	0.75
15	12.48	13.47	14.19	1.71	0.72	0.98
16	12.67	13.96	14.66	1.99	0.70	1.29
17	12.22	12.83	13.30	1.08	0.48	0.60
18	9.66	10.15	10.52	0.87	0.38	0.49
19	18.81	19.87	20.43	1.62	0.56	1.05
Average growth per year ($\text{mm m}^{-2} \text{ yr}^{-1}$)			0.26	0.27	0.25	
Standard deviation ($\text{mm m}^{-2} \text{ yr}^{-1}$)			0.11	0.10	0.12	

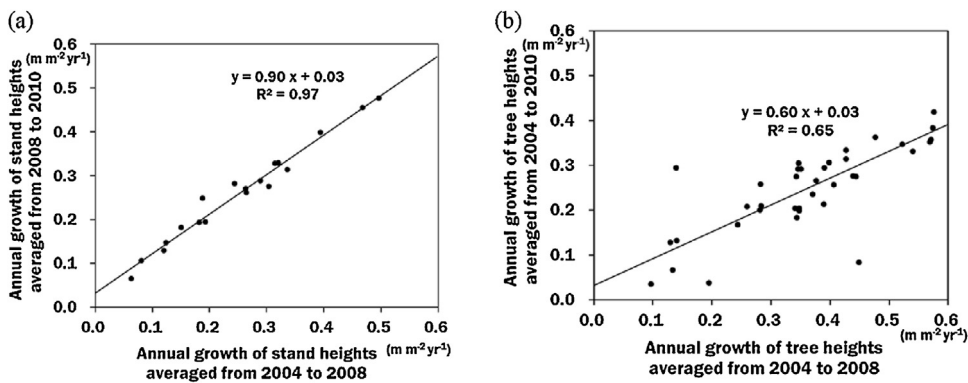


Fig. 2. LiDAR-estimated growing trends in (a) plot-based assessment ($N=19$) and (b) individual-tree-based assessment ($N=39$) between 2004 and 2008 and 2004 and 2010.

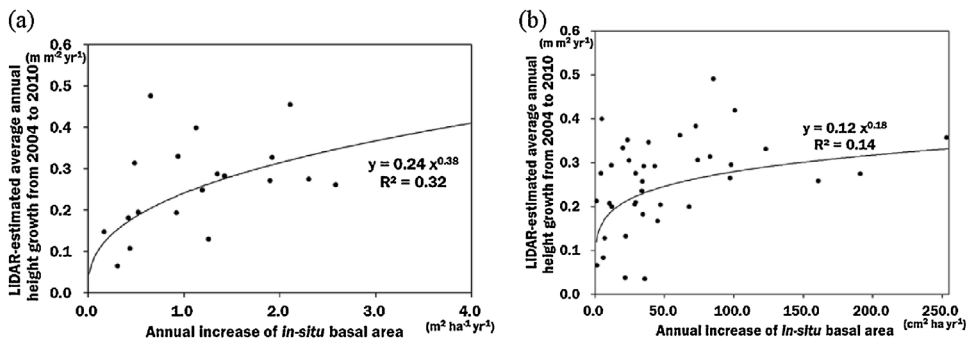


Fig. 3. The relation between LiDAR-estimated annual height growth and the increase of in situ basal area at the plot level (a) and at an individual-tree level (b).

Table 8

Pearson r between the LiDAR-estimated height growth and the increase of in-situ basal area.

	Increase of field-measured basal area	
	Plot level ($N=19$)	Individual tree level ($N=39$)
LiDAR-estimated growth	2004–2010	0.411*
	2008–2010	0.350*
	2004–2008	0.419*
		0.381**
		0.137**
		0.333**

* $p < 0.1$, grey character $p > 0.1$.

** $p < 0.05$.

3.2. Validation and the uncertainty of LiDAR estimations

Table 8 shows a significant and moderate linear relation between the LiDAR-estimated height growth and the increment of

the field-measured basal area (Pearson's $r=0.33\text{--}0.42$, $p < 0.1$). The relation is stronger in power regressions (Fig. 3). However, these weak correlations are a result of uncertainties in estimating canopy heights, as described in Fig. 4.

The ideal distribution of measurements in Fig. 4 appears above the 1:1 line, and the open circles indicate that heights in 2010 were shown at the highest, followed by filled circles (heights in 2008) and filled triangles (heights in 2004). Fig. 4a shows that the plot-level growth of average height through the study period follows the ideal trend, indicating the canopy heights in the order of 2010 (open circles) > 2008 (filled circles) > 2004 (filled triangles). This growing trend is also seen in Fig. 4b, for the growth of average tree height at the single-tree level. However, some of the trees were higher in 2008 than in 2010 (shown in the several filled circles higher than vertically corresponding open circles), whereas all the estimated heights in 2008 and 2010 were higher than the corresponding heights in 2004 (shown in all

Table 9

Average tree height at the plot level reported in Sasaki et al. (2007).

Plot ID	Field-measured average tree height (m)				Growth of field-measured tree heights per year (m yr^{-1})		
	1972 (at planting)	1982	1995	2004	1972–1982	1982–1995	1995–2004
1	1.0	4.3	6.7	6.4	0.33	0.18	-0.03
2	1.0	2.6	4.3	5.2	0.16	0.13	0.10
3	2.0	4.2	8.1	9.0	0.22	0.30	0.10
4	2.7	5.4	7.0	8.2	0.27	0.12	0.13
6	2.7	5.4	7.2	8.5	0.27	0.14	0.14
12	3.7	6.9	7.0	9.3	0.32	0.01	0.26
13	3.3	4.7	8.0	7.1	0.14	0.25	-0.10
14	2.8	5.9	6.5	7.6	0.31	0.05	0.12
15	3.5	4.5	7.3	8.3	0.10	0.22	0.11
16	3.5	5.1	7.6	8.9	0.16	0.19	0.14
17	2.5	6.2	8.8	9.6	0.37	0.20	0.09
18	2.5	4.9	7.9	8.9	0.24	0.23	0.11
Average value	2.6	5.0	7.2	8.1	0.24	0.17	0.10

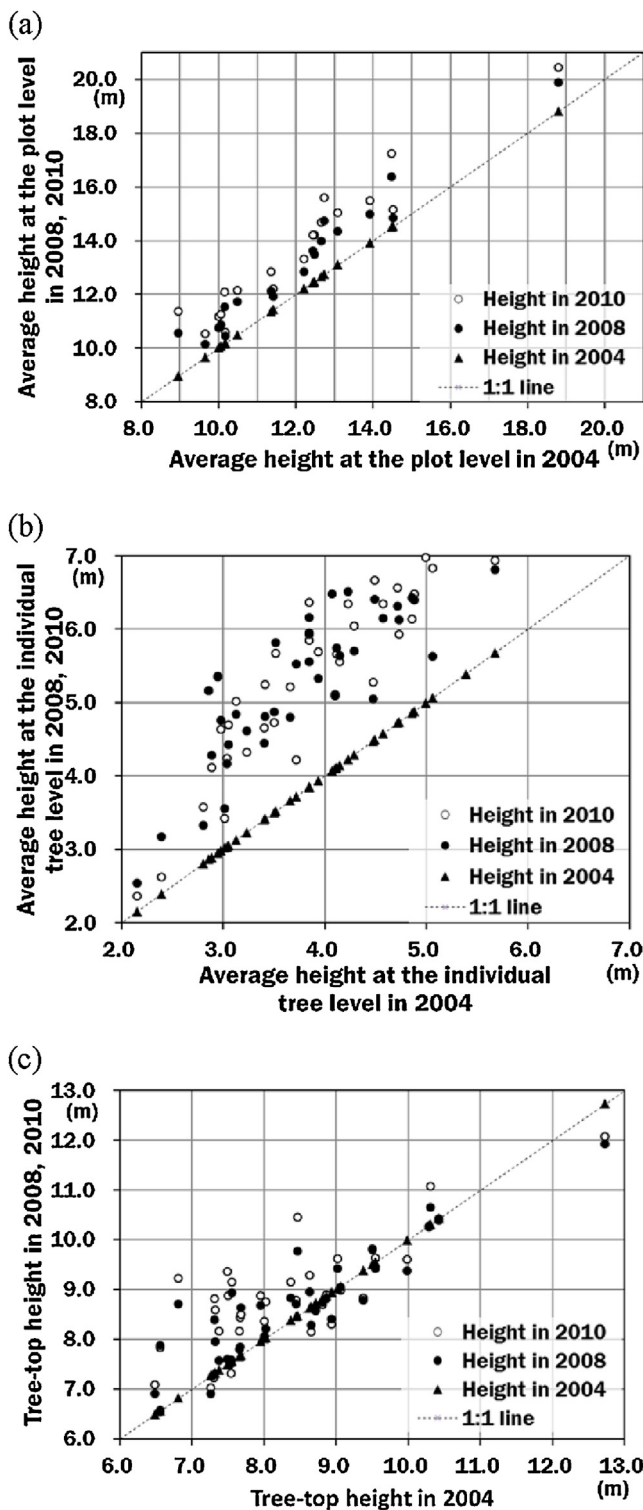


Fig. 4. Comparison of estimated canopy heights in 2004, 2008, and 2010, which were acquired from (a) the average heights in each plot area, (b) the averages, and (c) the maximum values (i.e., tree-top height) in each individual tree crown.

circles above the dashed 1:1 line with filled triangles). More of these uncertain cases were found in the estimation of tree-top height (Fig. 4c). The circles appearing below the 1:1 line imply the possibility that their heights in 2008 or 2010 decrease even lower than 2004.

4. Discussion

4.1. The growing trends

Consistent growing trends in the plot-level canopy heights (Table 5, Section 3.1) show a partial discrepancy with the result of a previous field survey (Sasaki et al., 2007) for the same corresponding plots, depending on the periods (Table 9). Field-measured heights of plants since 1972 in the selected long-term monitoring plots show the decrease in the annual growing trends, averaging from 0.24 m yr^{-1} during 1972–1982 to 0.10 m yr^{-1} during 1995–2004. However, note that this previous trend includes all the trees in the plots, not only the upper canopy layer but also the sub-canopy and understory trees. That might be the reason for the discrepancy between average field-measured tree heights in 2004 (Table 9) and LiDAR-estimated upper canopy heights in 2004 (Table 5). Considering the complex vertical structure of broad-leaved canopies, we focused on the change in the heights of upper-layer canopies rather than the change in sub-canopy stories. Canopy structures can be retrieved from the vertical distribution of LiDAR returns by use of statistical variables (e.g., percentile height, coefficient of variation, kurtosis, or skewness) (Jaskierniak et al., 2011; Næsset and Gobakken, 2005; van Aardt et al., 2006). However, Bater et al. (2011) argued against the reproducibility of sub-canopy structure retrieved by last returns, even in the condition of same-sensor specification and no forest dynamics, such as growth or gaps. Therefore, in using a multi-temporal LiDAR dataset acquired by different sensors and configurations, the LiDAR variables should be more stable in describing any changes of upper to lower canopy structure.

4.2. Causes of LiDAR-estimation uncertainty

The reasons of uncertainties in the growth estimation when LiDAR is used, particularly at the single-tree level (Section 3.2), seems to be based on following cases: (1) The uppermost part of the crown was missed. (2) The shoot elongation was not always in the vertical direction. (3) The specification of the LiDAR sensor was insufficient for detecting the apex within the crown. (4) The crown area was small, and accordingly the estimation accuracy per unit area was much more affected by the situations of (1)–(3) than by plot-level assessment. First, the branches in the upper canopy can be easily broken by strong wind, heavy rain, snow, or birds. In such case, the tree-top height is not always higher in the latest year than in previous years. Second, because not every growth of shoots elongates vertically, they do not always result in the increase of tree-top height (Yu et al., 2004). This tendency can be seen more in broad-leaved canopy than in conifers because of the relatively irregular crown shape. Third, the detection accuracy of LiDAR for the tree-top depends on the sensor performance, such as the sampling density of laser returns, the size of the laser footprint, and the threshold to record the laser signal as a return (Bater et al., 2011). Moreover, the LiDAR may find it difficult to detect the tree-top if the uppermost part consists of low-density leaves with sparse shoots. Last, these uncertain parts have more influence on the accuracy of estimating individual-tree heights than plot-scale heights, because the uncertainty per unit area caused by cases (1)–(3) appears remarkable when the estimation area is small (Section 3.2).

4.3. Lateral canopy growth

The growth estimation in this study was limited in the changes of CHMs in vertical direction, although trees grow in various directions. But the growth in lateral direction is also clearly shown in the image for calculating the difference in CHMs (Fig. 5). The boundary of crowns shown with high difference values in Fig. 5b may be the

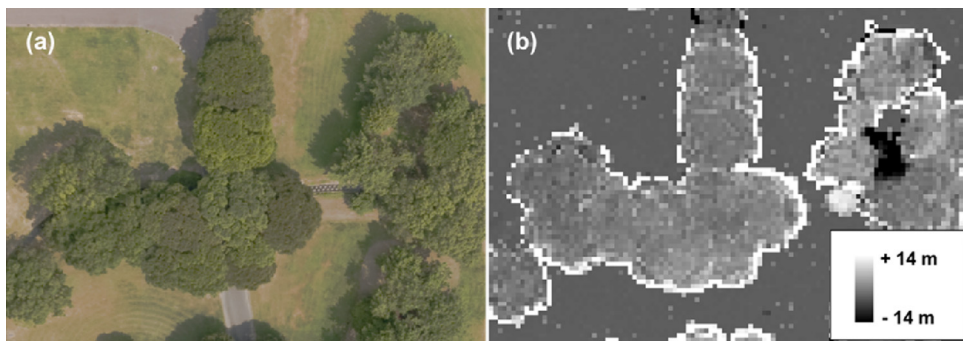


Fig. 5. Example of lateral growth and gap shown in the difference between LiDAR-derived canopy height models (CHMs) in 2004 and 2010. (a) Airborne image in true color. (b) Image obtained by CHM in 2010 minus CHM in 2004.

result of shoot elongation in the lateral direction during 2004 to 2010. On the contrary, the “minus growth” part indicates a gap (St-Onge and Vepakomma, 2004; Vepakomma et al., 2008), probably created when a large branch was broken.

To exclude those pixels where the value is unacceptable as vertical growth, the crown area for growth assessment should be carefully identified by referring to the image in former year and filtering those exceptions with an adequate threshold (Yu et al., 2004). However, these object- and site-specific situations remain as some of the limitations in growth assessment, especially in large-scale processing. Vepakomma et al. (2008) underlined the importance of LiDAR-detected lateral growth in monitoring gap dynamics, because it clearly showed the temporal changes at the gap edge in boreal coniferous forests. Therefore, the broad-scale LiDAR data analysis should be focused on how to incorporate the growth in the other direction with the vertical change at the single-tree level, as well as at the stand level in the case of a broad-leaved canopy.

5. Conclusion

This study assessed the vertical growth of broad-leaved canopies from the difference in CHMs derived by multi-year LiDAR datasets. Trends in the LiDAR-estimated growth of average canopy height agreed well with one another over the study periods at the individual-tree level as well as at the plot level, except for the short-term assessment from 2008 to 2010 of the single-tree growth. The LiDAR-estimated growth was validated by a moderate and significant relation with the increment of field-measured basal area, although larger uncertainties remained in the estimates at the individual-tree level than at the plot level. This may be the result of the tree-top part being broken by agents such as by wind or birds, the growth was not always in the vertical direction but in the lateral direction, or the performance of LiDAR was inadequate to detect the apex of the tree crown (i.e., tree-top height). Despite this limitation, LiDAR-estimated growth still has high potential in monitoring canopy growth and gap dynamics on a large scale and in providing key spatial information for the management of forested areas. Future study may apply these multi-LiDAR datasets to monitoring changes in aboveground biomass or canopy structure on a broad scale.

Acknowledgements

We acknowledge the staff of the Commemorative Organization for the Japan World Exposition '70 for their support in the field observation. This research was partly financed by the Commemorative Organization for the Japan World Exposition '70. Youngkeun Song acknowledges the support from BK21 Plus Project since 2014 (Seoul National University Interdisciplinary Program in

Landscape Architecture, Global Leadership Program Towards Innovative Green Infrastructure).

References

- Bater, C.A., Wulder, M., Coops, N.C., Nelson, R.F., Hilker, T., Næsset, E., 2011. *Stability of sample-based scanning-LiDAR-derived vegetation metrics for forest monitoring*. IEEE Trans. Geosci. Remote Sens. 49, 2385–2392.
- Brandtberg, T., 2007. *Classifying individual tree species under leaf-off and leaf-on conditions using airborne LiDAR*. ISPRS J. Photogramm. Remote Sens. 61, 325–340.
- Dean, T.J., Cao, Q.V., Roberts, S.D., Evans, D.L., 2009. *Measuring heights to crown base and crown median with LiDAR in a mature, even-aged loblolly pine stand*. For. Ecol. Manage. 257, 126–133.
- Dobbertin, M., 2005. *Tree growth as indicator of tree vitality and of tree reaction to environmental stress: a review*. Eur. J. For. Res. 124, 319–333.
- Hogg, E.H., Brandt, J.P., Kochtubajda, B., 2005. *Factors affecting interannual variation in growth of western Canadian aspen forests during 1951–2000*. Can. J. For. Res. 35, 610–622.
- Holmgren, J., Persson, A., 2004. *Identifying species of individual trees using airborne laser scanner*. Remote Sens. Environ. 90, 415–423.
- Hopkinson, C., Chasmer, L., Hall, R.J., 2008. *The uncertainty in conifer plantation growth prediction from multi-temporal LiDAR datasets*. Remote Sens. Environ. 112, 1168–1180.
- Jaskierniak, D., Lane, P.N.J., Robinson, A., Lucieer, A., 2011. *Extracting LiDAR indices to characterise multilayered forest structure using mixture distribution functions*. Remote Sens. Environ. 115, 573–585.
- Koukoulas, S., Blackburn, G.A., 2005. *Mapping individual tree location, height and species in broadleaved deciduous forest using airborne LiDAR and multi-spectral remotely sensed data*. Int. J. Remote Sens. 26, 431–455.
- Morimoto, Y., Njoroge, J.B., Nakamura, A., Sasaki, T., Chihara, Y., 2006. *Role of the EXPO '70 forest project in forest restoration in urban areas*. Landscape Ecol. Eng. 2, 119–127.
- Næsset, E., 1997. *Determination of mean tree height of forest stands using airborne laser scanner data*. ISPRS J. Photogramm. Remote Sens. 52, 49–56.
- Næsset, E., Økland, T., 2002. *Estimating tree height and tree crown properties using airborne scanning laser in a boreal nature reserve*. Remote Sens. Environ. 79, 105–115.
- Næsset, E., Gobakken, T., 2005. *Estimating forest growth using canopy metrics derived from airborne laser scanner data*. Remote Sens. Environ. 96, 453–465.
- Poage, N.J., Tappeiner, J.J.C., 2002. *Long-term patterns of diameter and basal area growth of old-growth Douglas-fir trees in western Oregon*. Can. J. For. Res. 32, 1232–1243.
- Popescu, S.C., 2007. *Estimating biomass of individual pine trees using airborne LiDAR*. Biomass Bioenergy 31, 646–655.
- Popescu, S.C., Zhao, K., 2008. *A voxel-based LiDAR method for estimating crown base height for deciduous and pine trees*. Remote Sens. Environ. 112, 767–781.
- Popescu, S.C., Wynne, R.H., Nelson, R.F., 2002. *Estimating plot-level tree heights with LiDAR: local filtering with a canopy-height based variable window size*. Comput. Electron. Agric. 37, 71–95.
- Reich, P.B., Teskey, R.O., Johnson, P.S., Hinckley, T.M., 1980. *Periodic root and shoot growth in oak*. For. Sci. 26, 590–598.
- Sasaki, T., Morimoto, Y., Imanishi, J., 2007. *The stand structure and soil properties of the forested area in a large scale reclamation site for 30 years after construction*. J. Jpn. Inst. Landscape Archit. 70, 413–418 (in Japanese with English abstract).
- Song, Y., Imanishi, J., Hashimoto, H., Morimura, A., Morimoto, Y., Kitada, K., 2013. *Spectral correction for the effect of crown shape at the single-tree level: an approach using a LiDAR-derived digital surface model for broad-leaved canopy*. IEEE Trans. Geosci. Remote Sens. 51, 755–764.
- St-Onge, B., Vepakomma, U., 2004. *Assessing forest gap dynamics and growth using multi-temporal laser-scanner data*. In: International conference NATSCAN 'Laser-Scanners for Forest and Landscape Assessment—Instruments, Processing Methods and Applications', 3–6 October 2004, Freiburg, Germany.

- pp. 173–178 (International Archives of Photogrammetry, Remote Sensing and Spatial Information Sciences, XXXVI, 8/W2).
- Takahashi, K., 2003. Effects of climatic conditions on shoot elongation of alpine dwarf pine (*Pinus pumila*) at its upper and lower altitudinal limits in Central Japan. *Arct. Antarct. Alp. Res.* 35, 1–7.
- Tappeiner, J.C., Huffman, D., Marshall, D., Spies, T.A., Bailey, J.D., 1997. Density, ages, and growth rates in old-growth and young-growth forests in coastal Oregon. *Can. J. For. Res.* 27, 638–648.
- van Aardt, J.A., Wynne, R.H., Oderwald, R.G., 2006. Forest volume and biomass estimation using small-footprint LiDAR-distributional parameters on a per-segment basis. *For. Sci.* 52, 636–649.
- Vepakomma, U., Kneeshaw, D., St-Onge, B., 2010. Interactions of multiple disturbances in shaping boreal forest dynamics: a spatially explicit analysis using multi-temporal LiDAR data and high-resolution imagery. *J. Ecol.* 98, 526–539.
- Vepakomma, U., St-Onge, B., Kneeshaw, D., 2008. Spatially explicit characterization of boreal forest gap dynamics using multi-temporal LiDAR data. *Remote Sens. Environ.* 112, 2326–2340.
- Vepakomma, U., St-Onge, B., Kneeshaw, D., 2011. Response of a boreal forest to canopy opening: assessing vertical and lateral tree growth with multi-temporal LiDAR data. *Ecol. Appl.* 21, 99–121.
- Waring, R.H., Thies, W.G., Muscato, D., 1980. Stem growth per unit of leaf area: a measure of tree vigor. *For. Sci.* 26, 112–117.
- Yu, X., Hyppä, J., Kaartinen, H., Maltamo, M., 2004. Automatic detection of harvested trees and determination of forest growth using airborne laser scanning. *Remote Sens. Environ.* 90, 451–462.
- Yu, X., Hyppä, J., Kukko, A., Maltamo, M., Kaartinen, H., 2006. Change detection techniques for canopy height growth measurements using airborne laser scanner data. *Photogramm. Eng. Remote Sens.* 72, 1339–1348.